

## 7. Discussion of a few room-temperature experiments

### 7.1. Single-molecule enzymatic dynamics

H. P. Lu, L. Xun, X. S. Xie, *Science* 282 (1998) 1877.

The enzyme cholesterol oxidase (COx) has two forms :

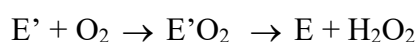
- an oxidised form, which is naturally fluorescent via its active site
- a reduced form, which is dark.

The 520 nm fluorescence of single COx molecules is collected in a confocal microscope with sample scanning and a detection yield of 10%. The molecules show a remarkable photostability. They emit up to 20 million photons, which is better than many dyes in water solution. This stability is attributed to the rigidity of the protein backbone protecting the active site.

Without cholesterol, the molecules can be detected in a microscope image, and they are stable. Upon reaction with its substrate (cholesterol), COx switches between the two redox forms. With low cholesterol concentration, the fluorescence shows blinking (clear on-off switching). The authors have checked that the blinking is related to individual redox reactions (blinking is independent on intensity, average turnover rate identical to that observed in bulk experiments). The histogram of the on-times (i.e. the lifetime of the oxidised form) shows a clear maximum, which indicates a waiting-time before the enzyme is reduced. This is due to a Michaelis-Menten mechanism :



with rates  $k_1$  of formation of the complex ES, and  $k_2$  of reaction leading to the product P. The enzyme E is a catalyst, regenerated in a second oxidative reaction :



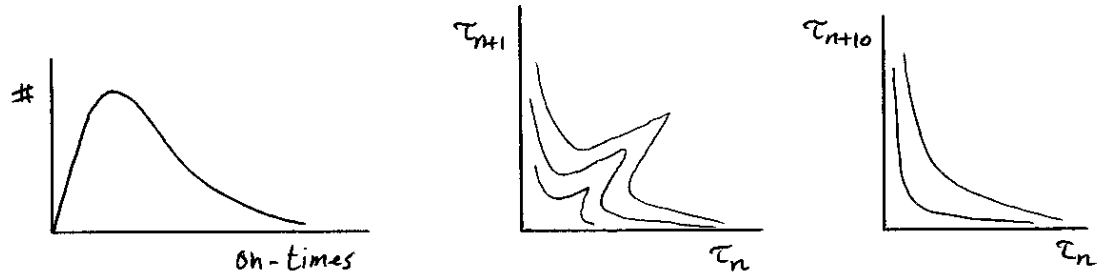
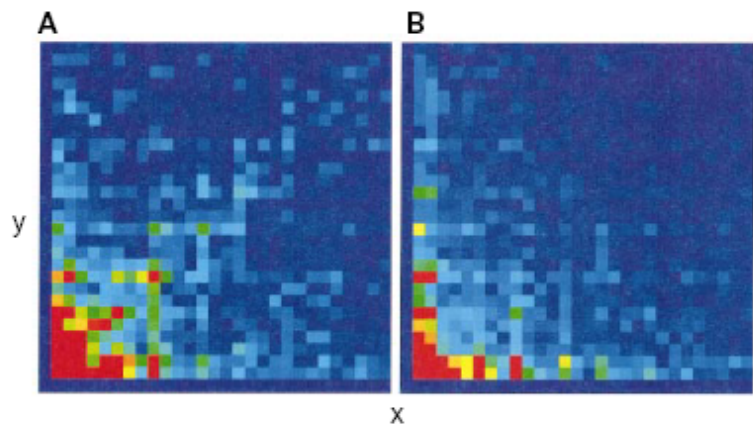


Figure 7.1 : Left : histogramme of the on-times showing a maximum : there is a waiting time before the enzyme is reduced. Center and left : correlation of consecutive on-times and absence of correlation of on-times separated by 10 off-times (excerpted with permission from Lu et al., Science 282 : 1877 (1998). Copyright 1998 AAAS).

Fig. 3. The 2D conditional probability distribution for a pair of on-times ( $x$  and  $y$ ) separated by a certain number of turnovers. The scale of  $x$  and  $y$  axes are from 0 to 1 s. (A) The 2D conditional histogram for on-times of two adjacent turnovers, which is derived from the trajectories of 33 COx molecules with 2 mM 5-pregene-3 $\beta$ -20 $\alpha$ -diol substrate. A subtle diagonal feature is present. (B) The 2D conditional histogram for two on-times separated by 10 turnovers for the COx molecules in (A). The diagonal feature vanishes because the two on-times become independent of each other at the 10-turnover separation. The color code in (A) and (B) represents the occurrence ( $z$  axis) from 350 (red) to 0 (purple).



The duration of an on-time corresponds to a reaction of the complex, therefore, the on-time histogram is given by the population of the complex as a function of time.

The solution of the rate equations gives :

$$p_{on}(t) = \frac{A}{k_2 - k_1} \left( e^{-k_1 t} - e^{-k_2 t} \right).$$

Depending on the larger of  $k_1$  and  $k_2$ , the rise time describes the formation of the complex by reaction of the enzyme and the decay time the reaction of the complex, or vice-versa.

The authors find evidence for non-exponential decay of the correlation function, which deviates from the single-exponential blinking model deduced from rate equations.

In addition, they found a correlation between consecutive on-times, which points to a molecular « memory » of the enzyme, and could be described by slow conformational changes. On-times separated by ten off-times were uncorrelated.

## 7.2. A single-molecule study of RNA catalysis and folding

X. Zhuang, L. E. Bartley, H. P. Babcock, R. Russell, T. Ha, D. Herschlag, S. Chu, Science 288 (2000) 2048.

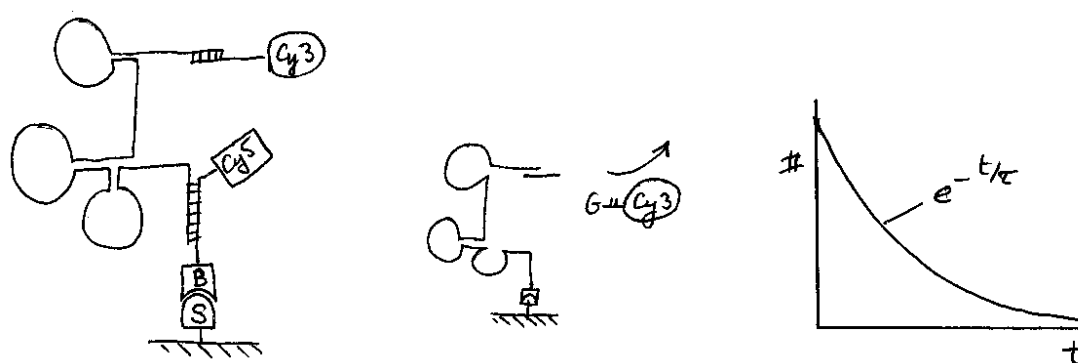


Figure 7.2 : Left : schematic representation of the ribozyme attached to a solid slide by a fluorescent, acceptor link. The end of the RNA strand is attached to a labelled substrate molecule (an oligonucleotide) by a different, donor dye. When the enzyme works in the presence of guanosine (G), it cuts the substrate and releases the label. The number of fluorescent RNA's decreases exponentially with reaction time (right).

In this work, RNA strands are attached to surfaces and labelled by one or two labels (Cy3 and Cy5). Images of a large number of single molecules immobilized on a surface are imaged by scanning confocal or by TIR microscopies. First, the functionality of the labelled and attached molecules was checked, by comparing a bulk solution measurement to single molecules. The RNA strand acts as an enzyme (ribozyme), that cleaves an oligopeptide (called the substrate, a short RNA strand). Labelled substrates were let to associate with the bound ribozyme, then the release of the label was monitored while guanosine (necessary for the reaction to take place) was introduced in the solution. The number of labelled molecules decayed exponentially, and the rate varied in the expected way as a function of guanosine concentration.

The next experiments exploited FRET between the two labels, one, the acceptor Cy5 attached to the link binding the ribozyme to the surface, the other, the donor Cy3

attached to the substrate (as earlier). The FRET efficiency varied from 0.9 to 0.3 between the docked and undocked states. The reversible docked-undocked equilibrium appeared as sudden FRET efficiency changes. A chemical modification of the substrate reduced the stability of the docked state, but not that of the transition state that leads to this state. This is shown by the invariable dwell time in the undocked state, while the dwell time in the docked state is reduced by a factor 10. The ribozyme tries to dock at the same rate, but can't stay in the docked state.

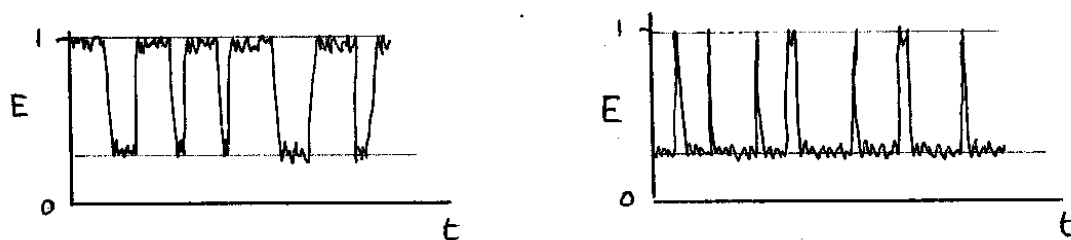


Figure 7.3 : FRET efficiencies as functions of time, showing transitions between docked (high  $E$ ) and undocked (low  $E$ ) states. When the substrate is chemically modified, the docked state is much less stable (right), but the stability of the transition complex is not affected.

A new and rare pathway for folding was found, which would have been difficult in ensemble measurements.

### 7.3. Single-molecule imaging of L-type $\text{Ca}^{2+}$ channels in live cells

G. S. Harms, L. Cognet, P. H. M. Lommerse, G. A. Blab, H. Kahr, R. Gamsjäger, H. P. Spaink, N. M. Soldatov, C. Romanin, Th. Schmidt, *Biophys. J.* 81 (2001) 2639.

Calcium channels are membrane proteins sensitive to voltage, that open or close to  $\text{Ca}^{2+}$  ions. They are labelled with green fluorescent protein (GFP, or rather eYFP, a mutation), which has the advantage that it is expressed by the cell itself. Transfected live cells (i.e. genetically modified cells) expressing this protein are investigated in a wide-field fluorescence microscope. The fluorescence is collected by a  $\times 100$ ,  $\text{NA}=1.4$  immersion objective. eYFP is excited at 514 nm and the fluorescence detection yield is about 5%. The radius of the point-spread function is  $320 \pm 80$  nm. The difficulty of the experiment is background from autofluorescence of the cell, which is reduced by illumination at  $5 \text{ kW/cm}^2$  for 1 s. The successive images from the CCD are treated by software to identify individual molecules (with Gaussian fits) and reconstruct their diffusion trajectories.

Fluorescence correlation microscopy is done on the same cells. The decay is attributed to translational diffusion and to photobleaching, leading to the following expression :

$$g^{(2)}(\tau) = 1 + \frac{1}{N} \left( 1 + \frac{\tau}{\tau_D} \right)^{-1} e^{-\frac{\tau}{\tau_B}}$$

involving a diffusion time  $\tau_D$  (in two dimensions) and a bleaching time  $\tau_B$ .

Control experiments demonstrate that the signals indeed arise from single molecules : the intensity of the fluorescent spots matches that of immobilized eYFP molecules under the same conditions. The spots display one-step photobleaching, a common criterion for single-molecule signals. Some of the signals are highly polarized, a signature of immobilized single quantum systems (the other molecules are rotating fast). Single-molecule concentrations are consistent with FCS contrasts (giving about 10 mol./  $\mu\text{m}^2$ ).

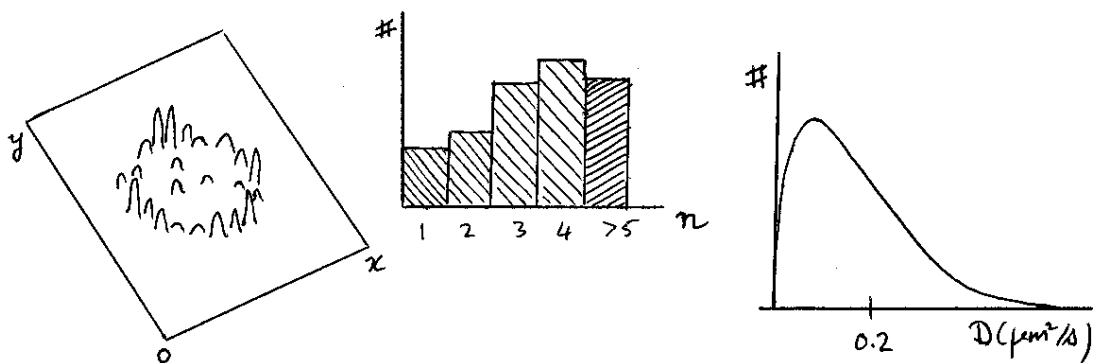


Figure 7.4 : Left : Distribution of fluorescently labelled ion channels in a living cell. Wide-field imaging produces a cut of the cell, showing that channels are mainly concentrated in the cell membrane. Center : histogram of the number of fluorescent label per spot, with a maximum for 3 to 4 channels. Right : histogram of diffusion coefficients for various molecules in the membrane, showing wide distributions of mobilities, probably related to aggregation.

The study shows clustering of the ion channels, with an average number of molecules of 40 per cluster. Due to preliminary bleaching, only 3 fluorescent labels on average are left when the diffusion experiment starts.

Mobility studies show that the ion channels are confined in the membrane, where diffusion is much slower ( $D = 0.15 \mu\text{m}^2 / \text{s}$ ) than in the cytosol ( $D = 20 \mu\text{m}^2 / \text{s}$ ).